





ARTICLE OPEN



Neuron enriched extracellular vesicles' MicroRNA expression profiles as a marker of early life alcohol consumption

Vasily Yakovlev^{1,6}[✉], Dana M. Lapato^{2,6}, Pratip Rana³, Preetam Ghosh³³, Rebekah Frye⁴⁴ and Roxann Roberson-Nay⁵⁵

© The Author(s) 2024

Alcohol consumption may impact and shape brain development through perturbed biological pathways and impaired molecular functions. We investigated the relationship between alcohol consumption rates and neuron-enriched extracellular vesicles' (EVs') microRNA (miRNA) expression to better understand the impact of alcohol use on early life brain biology. Neuron-enriched EVs' miRNA expression was measured from plasma samples collected from young people using a commercially available microarray platform while alcohol consumption was measured using the Alcohol Use Disorders Identification Test. Linear regression and network analyses were used to identify significantly differentially expressed miRNAs and to characterize the implicated biological pathways, respectively. Compared to alcohol naïve controls, young people reporting high alcohol consumption exhibited significantly higher expression of three neuron-enriched EVs' miRNAs including miR-30a-5p, miR-194-5p, and miR-339-3p, although only miR-30a-5p and miR-194-5p survived multiple test correction. The miRNA-miRNA interaction network inferred by a network inference algorithm did not detect any differentially expressed miRNAs with a high cutoff on edge scores. However, when the cutoff of the algorithm was reduced, five miRNAs were identified as interacting with miR-194-5p and miR-30a-5p. These seven miRNAs were associated with 25 biological functions; miR-194-5p was the most highly connected node and was highly correlated with the other miRNAs in this cluster. Our observed association between neuron-enriched EVs' miRNAs and alcohol consumption concurs with results from experimental animal models of alcohol use and suggests that high rates of alcohol consumption during the adolescent/young adult years may impact brain functioning and development by modulating miRNA expression.

Translational Psychiatry (2024)14:176; <https://doi.org/10.1038/s41398-024-02874-3>

INTRODUCTION

Adolescents and young adults frequently consume alcohol and often engage in binge drinking, making it the most used and misused substance among teens [1–3]. Although most young people who binge or heavily drink do not currently have an alcohol use disorder (AUD), these alcohol use (AU) patterns can lead to lasting neurobiological changes and an increased likelihood of developing an AUD [4–11]. The cellular processes underlying the effects of alcohol use and misuse in young people are not well understood.

A diverse array of molecular modifications, nucleic acids, and cellular machinery jointly regulate gene expression. Much attention has been paid to characterizing the intracellular biological pathways and actors that augment or repress messenger RNA (mRNA) abundance and protein production, which has led to an increased appreciation of the role of microRNAs. MicroRNAs (miRNA) are non-coding RNAs that coordinate with cellular machinery to finetune gene expression [12]. MiRNAs exhibit self-regulatory mechanisms, regulate the expression of other genes/miRNAs, and influence biological processes within cells. Although miRNA activity is present throughout the entire human life course, miRNAs play especially key roles during development,

differentiation, and cell-fate determination [12]. Additional evidence suggests that miRNAs serve as key roles in immune system functioning, aging, and reproduction.

Several preclinical studies and a few human studies have investigated microRNAs (miRNAs) in the context of alcohol use. These studies reveal miRNAs that map to genes related to hypothesized etiologic alcohol use pathways, including neuroplasticity/brain development and immune system/inflammation [13–23]. For instance, in human post-mortem brain samples, approximately 35 miRNAs exhibited differential expression levels in the prefrontal cortex (PFC) of adult humans who abused alcohol compared to controls and over-expression of miRNAs was inversely associated with the expression of their target mRNAs [24]. Robust changes in miRNA expression also have been reported in the brains of rodents following chronic alcohol exposure, with ~41 rat miRNAs being significantly altered in the medial PFC [25]. Gene ontology results indicated that differential expression was related to functional processes commonly associated with neurotransmission, synaptic plasticity, and neuroadaptation. In a study comparing persons with AUDs to non-drinking controls, increased expression was found for mir-96, mir-24, and mir-136 and decreased mir-92b expression in persons with

¹Department of Radiation Oncology, Massey Cancer Center, Virginia Commonwealth University, Richmond, VA, USA. ²Department of Human and Molecular Genetics, School of Medicine, Virginia Commonwealth University, Richmond, VA, USA. ³Department of Computer Science, College of Engineering, Virginia Commonwealth University, Richmond, VA, USA. ⁴Neuroscience Program, School of Medicine, Virginia Commonwealth University, Richmond, VA, USA. ⁵Department of Psychiatry, School of Medicine, Virginia Commonwealth University, Richmond, VA, USA. ⁶These authors contributed equally: Vasily Yakovlev, Dana M. Lapato. [✉]email: vasily.yakovlev@vcuhealth.org

Received: 14 August 2023 Revised: 11 March 2024 Accepted: 13 March 2024

Published online: 04 April 2024

AUDs [26]. These findings are consistent with human and animal studies of brain tissue [27–30]. Moreover, the observation of primarily increased levels among persons with AUDs is in agreement with the findings from post-mortem brain tissue derived from persons suffering from alcohol use disorder [24] and suggests the presence of a potential compensatory mechanism in response to neuronal damage or, possibly, an intensified transfer of miRNAs from the brain to the peripheral regions due to cellular harm [26]. Thus, miRNA expression may hold great potential to elucidate pathways to alcohol-induced brain alterations and damage [31, 32].

Given that all miRNAs are not thought to participate equally in every biological function or developmental process, it is not surprising that miRNAs vary considerably in expression levels [33] and that these levels almost certainly vary by sex, age, health status, and environmental (e.g., exposure to pollution) and behavioral (e.g., substance use) factors. Most importantly, miRNAs can be shuttled through the bloodstream by extracellular vesicles (EVs). EVs are robust biological sacs that transport cargoes of proteins, RNAs (including miRNAs), DNA, and lipids throughout the body and across the blood-brain barrier. This portability enables brain-derived EVs to be isolated from peripheral blood, opening a window to the brain by identifying, quantifying, and characterizing EV cargo throughout the lifespan to understand both normal physiology and pathophysiology [34].

The current study investigated the abundance and potential roles of circulating EVs during adolescence/young adulthood. EVs have been associated with a wide range of conditions, including neurodegenerative disorders and cancer [35–40]. The majority of EV research has focused exclusively on adult populations, leaving significant knowledge gaps regarding the number, type, and cargo content of EVs in healthy children, adolescents, and young adults and whether perturbations in any of these characteristics could be concomitant with, predict, or follow significant changes in health, development, or functioning. For the cargo analysis, we prioritized miRNAs in the EV cargo analysis given that miRNAs serve prominent roles in brain functioning and development [41], are relatively abundant in many EVs, and are amenable to high throughput measurement. Additionally, miRNAs are inherently biologically active. Unlike mechanisms like DNA methylation, which may or may not be directly impacting expression profiles of the genic regions it overlaps, miRNAs are mobile and capable of associating with targets and partner cellular machinery from the moment that they exit EVs and enter recipient cells. Moreover, robust methods and resources [33] exist to identify, quantify, and characterize miRNAs and their functionality, making miRNAs more tractable candidates for gene network analyses than more enigmatic and less well-characterized options like long noncoding RNAs.

MATERIALS AND METHODS

Participants

All specimens and participant data used in this study were collected as part of the Adolescent and Young Adult Twin Study (AYATS; R01MH101518; IRB protocol #HM20022942) and recruited primarily through the Mid-Atlantic Twin Registry. The informed consent was obtained from all subjects. AYATS included two study visits separated by two years. Young people reporting high alcohol consumption rates (i.e., AUDIT-C ≥ 6) were selected for inclusion. Given that alcohol use rates are highly correlated among twin pairs, this resulted in 5 twin pairs being included in the AU case group, with the remaining 12 alcohol cases being individuals. All control participants were individuals (i.e., no twin pairs). We excluded participants who reported any major medical conditions (such as liver or kidney dysfunction, cardiovascular disease, etc.). Thus, our sample of adolescents/young adults was generally healthy.

During each visit, participants completed self-report questionnaires and provided blood samples. Self-report questionnaires queried youth regarding multiple domains including psychiatric conditions, personality, social relations, and substance use. Blood samples were spun down to separate the plasma, which was stored at -80°C .

Alcohol consumption

The Alcohol Use Disorders Identification Test (AUDIT) was developed by the World Health Organization and is the most widely used alcohol screening instrument of past-year alcohol use patterns [42–50]. The test consists of 10 items across three dimensions including consumption (termed AUDIT-C), dependence, and problematic or hazardous alcohol use. A meta-analysis found the 3-item AUDIT-C to be as effective as the full 10-item AUDIT in screening for at-risk drinking and AUDs. Responses to each of the three questions are assigned 0–4 points, yielding a total score of 0–12. AUDIT-C screening thresholds that optimize sensitivity and specificity for detecting unhealthy alcohol use are ≥ 4 in males and ≥ 3 in females [45] whereas a study of adolescents suggested a cutoff score of ≥ 3 as indicative of problematic alcohol use for males and females [42]. AUDIT-C scores will serve as the primary AU variable given that we are most interested in the impact of alcohol consumption rates on the brain neurobiology of young people.

Short mood and feelings questionnaire (SMFQ)

The SMFQ is a 13-item questionnaire that maps onto DSM criteria for depression, with a total range of 0–26. The time frame for answering the SMFQ is the past two weeks and a total score greater than 12 may indicate the presence of depression. The SMFQ is a well validated measure normed for adolescents [51–53].

Smoking behaviors

Use of combustible cigarettes, electronic cigarettes, and marijuana was assessed. Given that no one smoking behavior was endorsed with high frequency, all three behaviors were aggregated to generate a single index of smoking behaviors. The smoking behavior variable was coded as binary (0=no smoking behaviors endorsed, 1=one or more smoking behaviors endorsed).

EVs isolation and enrichment

EVs were extracted from plasma samples by size exclusion chromatography method using the qEVoriginal columns (Izon Science). Every 0.5 ml of plasma yielded 1.5 ml of purified EVs in the 1xPBS buffer. EVs precipitation was performed overnight at $+4^{\circ}\text{C}$ on a rotating mixer with L1CAM/CD171 Monoclonal Biotin Conjugated Antibody (eBio5G3 (5G3), ThermoFisher) in the presence of 3% BSA and 3x Proteinase/Phosphatase Inhibitors cocktail (Sigma-Aldrich). After overnight incubation samples were additionally incubated with Pierce™ Streptavidin Plus UltraLink™ Resin (ThermoFisher) for 1 h at $+4^{\circ}\text{C}$. As a washing step, sample tubes were centrifuged with $500 \times g$ for 1 min, the supernatant was removed and saved as non-neuronal fraction of plasma EVs, and resin beads were washed 3x times with cold 1 ml of pre-filtered (with 0.22 μM filter) 1xPBS buffer. After final wash, precipitated neuronal-enriched EVs were eluted by incubation of the Streptavidin beads with 100 μl of Pierce™ IgG Elution Buffer (ThermoFisher) at room temperature with mixing for 5 min. As a negative control, EVs precipitation was performed with biotin-conjugated IgG2a kappa Isotype Control (eBM2a, ThermoFisher).

Nanoparticle tracking analysis

The concentration and size of EVs were measured using ZetaView® Nanoparticle Tracking Analysis. All samples were diluted in PBS to a final volume of 2 ml. Ideal measurement concentrations were found by pre-testing the ideal particle per frame value (140–200 particles/frame). The manufacturer's default software settings for EVs were selected accordingly. For each measurement, three cycles were performed by scanning 11 cell positions each and capturing 80 frames per position under following settings: Focus: autofocus; Camera sensitivity for all samples: 78; Shutter: 100; Scattering Intensity: detected automatically; Cell temperature: 25°C . After capture, the videos were analyzed by the in-built ZetaView Software 8.04.02 SP2 with specific analysis parameters: Maximum area: 1000, Minimum area 5, Minimum brightness: 25. Hardware: embedded laser: 40 mW at 488 nm; camera: CMOS. The number of completed tracks in NTA measurements was always greater than the proposed minimum of 1000 to minimize data skewing based on single large particles.

Western blot analysis

For protein analysis all samples were loaded and separated by SDS-PAGE gel and transferred to nitrocellulose membranes. The membranes were exposed to antibodies at specific dilutions. Primary antibodies used for WB:

anti-L1CAM(CD171) (dilution 1:1000, ThermoFisher), anti-CD63 (dilution 1:1000, ThermoFisher), anti-TSG101 (dilution 1:500, Cell Signaling), anti-Albumin (dilution 1:1000, Cell Signaling). Specific protein bands were detected using infrared-emitting conjugated secondary antibodies: anti-rabbit DyLight™ 800 4X PEG Conjugate (dilution 1:10,000, Cell Signaling). WB images were generated and analyzed using the ChemiDoc Infrared Imaging System (Bio-Rad).

Transmission electron microscopy (TEM)

Isolated EVs were fixed and prepared for the TEM as was previously described [54]. The TEM analysis was carried out by the Microscopy Core of VCU.

EVs RNA isolation and RT-PCR

Total RNA was isolated from the EV samples following the manufacturer's instructions with the miRNeasy MicroRNA Extraction Kit (Qiagen) and then converted to cDNA using the miRCURY LNA RT Kit (Qiagen). The samples with total EVs RNA and cDNA were stored in a freezer at -80°C . The concentration and purity of the EVs RNA samples were estimated using NanoDrop ND-1000 spectrophotometer (Thermo Scientific, Wilmington DE).

All cDNA samples were pooled into two groups corresponding to cases (alcohol drinkers) and controls (non-drinkers) and then assayed using the Serum/Plasma Focus PCR panel (Qiagen). This commercially available microarray platform contains 179 LNA miRNA primer sets of miRNAs that have been commonly found in human plasma. The Serum/Plasma Focus miRNA PCR Panels include potential reference genes and probes for evaluating potential sample contamination or damage (e.g., hemolysis). Each PCR panel also contains set of the negative control (H_2O) and five sets of RNA Spike-In controls to evaluate RNA extraction (Spike-Ins 2-4-5; concentration ratio 1:100:10000) and cDNA synthesis (Spike-In 6) and to perform inter-plate calibration (Spike-In 3). The amplification was performed in a QuantStudio 5 Real-Time PCR System (Thermo Fisher Scientific, USA). Samples were amplified using RT2 SYBR® Green qPCR Mastermix with ROX (carboxy-X-rhodamine) passive reference dye from QIAGEN. The real-time PCR data were normalized by ROX passive reference. The amplification curves were analyzed using the QuantStudio™ Design & Analysis Software v1.4.2, both for determination of Ct values and for melting curve analysis. All assays were inspected for distinct melting curves and the T_m was checked to be within known specifications for each assay. The $2^{-\Delta\Delta\text{Ct}}$ method was used for the calculation of relative miRNA expression levels.

RT-PCR data analysis

RT-PCR count data was imported into the R statistical environment [55]. Potential reference genes were identified by comparing the overall stability and relative expression of candidate miRNAs across cases and controls. MiRNAs that exhibited at least a 5-fold difference in expression between cases and controls were subsequently assayed in all individual participants using quantitative PCR. The individual-level miRNA expression values were imported in the R statistical environment where 21 multivariate linear regression analyses were conducted to test for an association between AU group and miRNA expression. Demographic factors (i.e., age, sex) served as covariates. We also included smoking behaviors and current depression symptoms as covariates given that these behaviors are frequently concomitant with AU in teens [56–66] and we included family id as a fixed effect to account for twin pair relatedness. Partial eta squared (η^2) was computed for all variables in the model. This effect size estimate reflects the proportion of variance explained by a variable in relation to the total variance, while accounting for the variance explained by the other variables in the model. A Bonferroni correction also was applied to correct for multiple testing (21 tests, $\alpha = 0.05$; Bonferroni adjusted $p \leq 0.002$).

Functional network analysis

We applied a network-based approach to analyze miRNA regulation and find potential miRNA biomarkers of alcohol consumption. We used the miRsig tool [67, 68] to infer the miRNA-miRNA interaction network. MiRsig tool operates by (1) collecting miRNAs expression in a disease/condition from multiple patients, (2) running six reverse-engineering network inference algorithms on the expression data to infer miRNA-miRNA interaction scores/probability, and (3) performing a consensus-based approach to get a more accurate network from these six miRNA-miRNA

Table 1. Demographic and clinical features of alcohol use groups.

	Alcohol Use Group		t/ χ^2	p
	Controls	Cases		
Age	18.1 (1.39)	19.7 (1.5)	-3.7	0.001
Sex, n (%) female	9 (50.0)	8 (33.3)	1.2	0.276
Race, n (%) Caucasian	18 (100)	24 (100)	---	---
Ethnicity, n (%) Latino	2 (11.1)	2 (8.3)	0.1	0.762
Smoking Behaviors, n (%)	0 (0.0)	10 (41.7)	9.8	0.002
SMFQ Total Score	3.8 (3.1)	6.2 (5.4)	1.6	0.110
AUDIT-C	0.0 (0.0)	8.0 (1.0)	8.0	<.001

interaction algorithm outputs. Each network inference algorithm has some individual bias, and their performance varies in different datasets. The consensus approach reduces the noise and prediction error by employing a consensus of six different algorithms as demonstrated by Nalluri et al. [67] GO analysis was performed using the miRNA set enrichment analysis tool known as TAM 2.0. The TargetScan database [69, 70] was used to predict the targets of miRNAs belonging to the revealed clusters. For the alcohol dependence-associated genes list, we utilized the GWAS database (<https://www.ebi.ac.uk/gwas/home>).

RESULTS

Participants

Table 1 provides summary statistics for demographic, smoking, and alcohol use variables by alcohol case-control status. Of the 44 participants selected for study inclusion, $n = 26$ (59%) endorsed alcohol consumption while $n = 18$ self-reported as not having initiated alcohol use in their lifetime. Two individuals were excluded from the analyses, with one excluded due to poor sample quality and the second participant for a nonqualifying AUDIT-C score (i.e., AUDIT-C = 2). These exclusions resulted in a final sample of 42 young people, with 24 classified as AU cases and the remainder as alcohol naive controls. AU cases reported high rates of alcohol consumption (i.e., Mean AUDIT-C = 8.0, $SD = 1.0$, range 6–10). The alcohol use groups did not differ on sex, race, ethnicity, or current depression symptoms (see Table 1). Young people classified as AU cases were older ($t = -3.7$, $p = 0.001$) and significantly more likely to endorse smoking behaviors, with approximately 42% reporting one or more smoking behaviors ($\chi^2 = 9.8$, $p = 0.02$).

Extraction of neuron-enriched EVs

Quality and quantity of total EVs extracted from plasma samples were analyzed by different methods. Ponceau S staining of the different fractions after size-exclusion chromatography showed a high purity of EV fractions with almost no contamination by plasma proteins (Fig. 1A). Most plasma proteins were isolated with late protein fractions #7–10. Western blot analysis demonstrated that only EV fractions contain EV-specific protein markers CD63 and TSG101 and, at the same time, showed no contamination with plasma albumin (Fig. 1B). Interestingly, the neuronal marker L1CAM (CD171) was revealed in EV fractions but not in the fractions of the plasma proteins. TEM analysis demonstrated that the EV fractions contain vesicles with the shape and size corresponding to 30–120 nm (Fig. 1C). Nanoparticle tracking analysis showed average concentration of EVs in plasma samples $3.1 \pm 0.8 \times 10^{11}$ (particles/ml) (Fig. 2A). After extraction from 0.5 ml of plasma sample, the EV fraction had a volume 1.5 ml with concentration $9.3 \pm 2.6 \times 10^{10}$ (particles/ml). Hence, we were able to extract and purify ~90% of plasma EVs. After precipitation with anti-L1CAM (CD171) Abs, neuron-enriched EVs were eluted in the

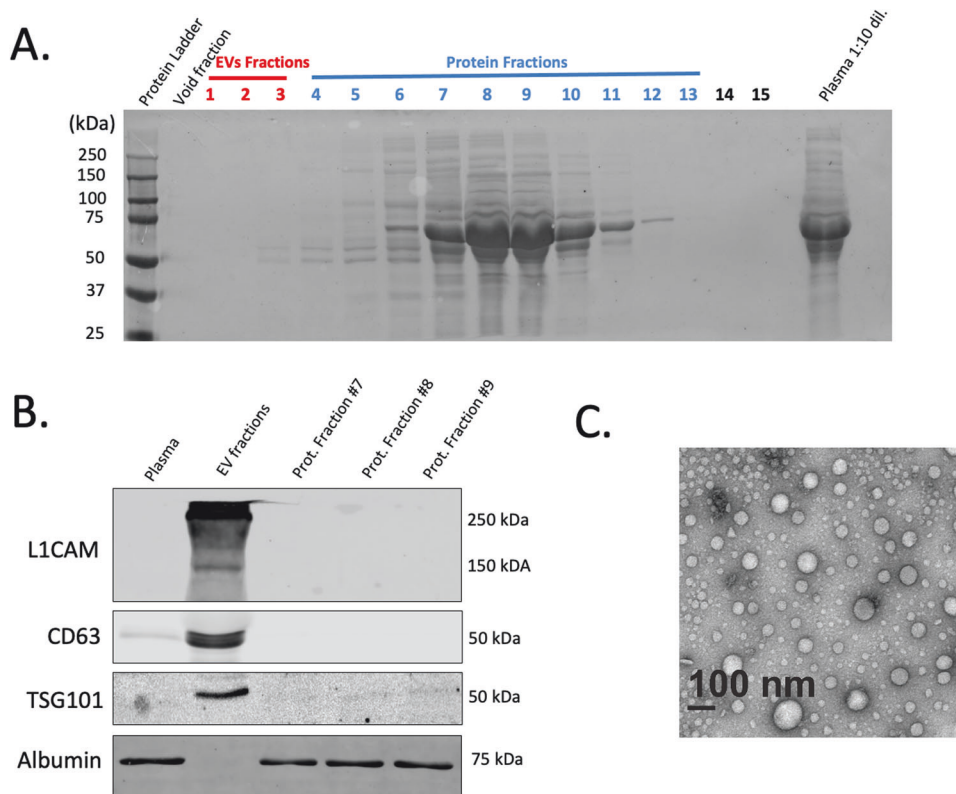


Fig. 1 Extraction and characterization of EVs from patient's plasma samples. **A** Ponceau S staining of the different plasma fractions after extraction of EVs by size-exclusion chromatography. **B** Western blot analysis of EV-specific protein markers. Equal amount of total protein was loaded for native plasma, combined EV fractions, and Protein fractions #7-9 (as shown in Fig. 1A). **C** Electron microscopy analysis for the extracted EVs.

0.2 ml of elution buffer and demonstrated concentration $2.6 \pm 0.7 \times 10^9$ (particles/ml). This result means that the neuron-enriched fraction of EVs accounted for 0.04% of the total number of EVs isolated from plasma. EV precipitation with the biotin-conjugated IgG2a kappa Isotype Control (negative control) demonstrated that, in the absence of specific anti-L1CAM(CD171) Abs, concentration of precipitated EVs was significantly lower ($1.2 \pm 0.3 \times 10^6$ particles/ml) (Fig. 2A). Western blot analysis confirmed that while neuron-enriched and non-neuron EVs expressed comparable levels of markers CD63 and TSG101, only neuron-enriched EVs have a distinguishable level of L1CAM (CD171) protein expression (Fig. 2B).

Analysis of miRNAs from neuron-enriched EVs

The group-based microarray analysis identified 104 miRNAs, 6 of which showed the most stable expression and were identified as a potential normalization controls: miR-126-5p, miR-133a-3p, miR-139-5p, miR-197-5p, miR-328-3p, miR-199a-5p. Analysis of these miRNAs in all individual samples revealed that the most stable expression was demonstrated by miR-133a-3p and miR-197-5p (Fig. S1). For further qPCR data analysis, miR-133a-3p was used as a normalization control. Out of 104 identified miRNAs, 22 showed at least a 50-fold difference in expression between heavy drinkers and controls. These 22 miRNAs were followed up with individual-level measurement via qPCR. One miRNA, mir-423-3p, produced unreliable qPCR measures and was removed from consideration. Analysis of individual samples showed no statistically significant difference between alcohol consumption and control groups for 18 out of the remaining 21 miRNAs (Fig. S2). As presented in Table 2 and Fig. 3, 3 of 21 miRNAs (miR-30a-5p, miR-194-5p, and miR-339-3p) were significantly differentially expressed by alcohol consumption group after controlling for age, sex, smoking

behaviors, current depression symptoms, and accounting for twin pair relatedness; however, only miR-30a-5p and miR-194-5p survived Bonferroni correction. Both miR-30a-5p and miR-194-5p exhibited large effect sizes, with partial eta squared values of 0.26 and 0.24, respectively. Although miR-339-3p did not meet Bonferroni corrected significance, this miRNA was associated with a medium effect size. Supplemental Table 1 presents unadjusted and covariate adjusted means and standard errors for the 21 miRNAs while Supplemental Table 2 provides linear model parameter estimates for AU group and covariates on expression levels for non-significant miRNAs ($p > 0.05$).

miRNA-miRNA interaction network inference

The miRNA-miRNA interaction network inferred by the miRsig tool for the alcohol consumption network is shown in Fig. 4A. This network consists of 16 miRNAs and 77 edges arranged in two connected clusters. None of the miRNAs in this predicted network were differentially expressed (DE) by case status. Let-7i-5p miRNA was found to be the highest-degree node in this network. For a sensitivity analysis, we recreated the miRNA-miRNA interaction network with only unrelated individuals by dropping one twin from each of the six twin pairs. No significant difference in the general network structure was observed after dropping these twins (Fig. 4B). Let-7i-5p was still ranked as the highest-degree node in the network, and the two networks shared 88% of their edges (61/69).

miRNAs interacting with DE miRNAs

Because none of the differentially expressed miRNAs from the regression models appeared in our initial miRNA-miRNA interaction network, we built another network with differentially expressed miRNAs and their direct regulators (neighbors in the

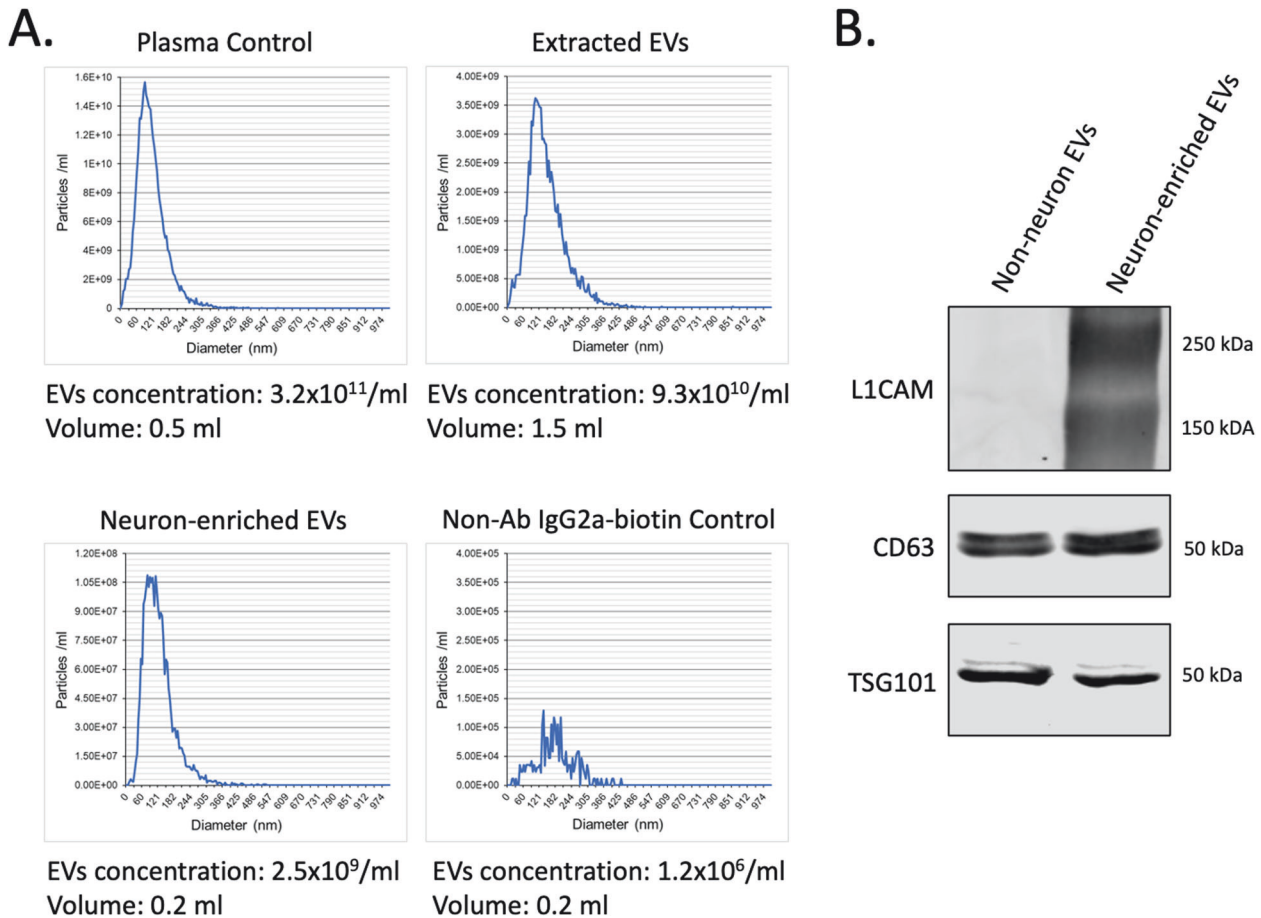


Fig. 2 **Precipitation and characterization of neuron-derived EVs.** **A** Nanoparticle tracking analysis of EVs in the native plasma (Plasma Control), after extraction from plasma by the size-exclusion chromatography (Extracted EVs), after precipitation with Anti-L1CAM(CD171) Ab (Neuron-enriched EVs), and after precipitation with the biotin-conjugated isotype control IgG2a (negative control). **B** Analysis of EV-specific markers and L1CAM(CD171) protein expression in neuron-derived EVs and non-neuronal EVs (supernatant). Equal amount of total protein from both samples were used for Western blot analysis.

network) by rerunning the miRsig pipeline with a reduced consensus cutoff (original cutoff 0.8, new cutoff 0.7) so that all the differentially expressed miRNAs would be included. This second network consisted of seven miRNAs thought to work together (Fig. 4C). A functional analysis identified 25 biological functions significantly associated with these miRNAs (Fig. 4D). miR-194-5p was ranked the highest-degree node in this network and its expression was highly correlated with the other miRNAs in this cluster (Fig. 4E).

We employed the TargetScan database to predict the targets of seven miRNAs belonging to the cluster depicted in Fig. 4C and the GWAS database was used to generate the alcohol dependence-associated genes list. The Table 3 presents the number of targets for all seven miRNA and the associated alcohol dependence and consumption gene targets.

DISCUSSION

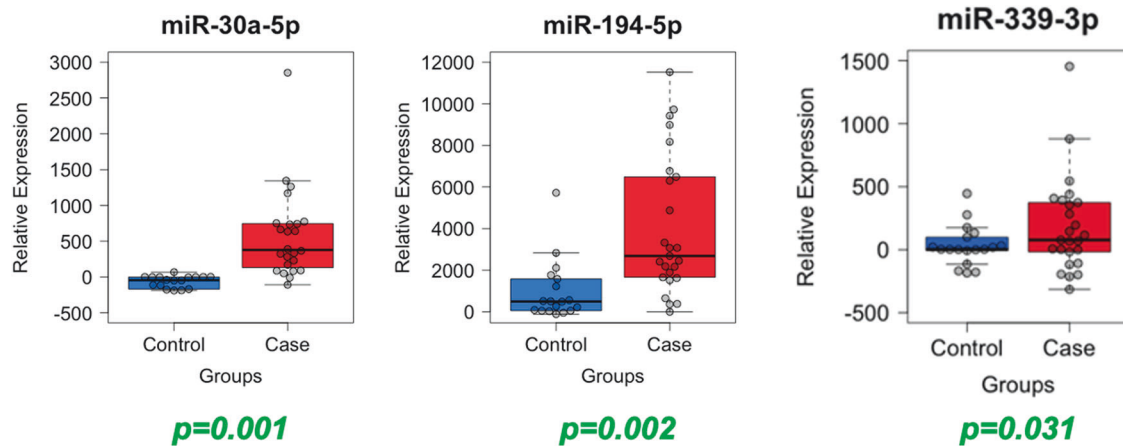
We used a commercially available microarray platform to identify neuron-enriched exosomal miRNAs differentially expressed by self-reported alcohol consumption rate in a healthy sample of young people. Follow up molecular studies validated the microarray results, and multivariate regression models controlling for demographics and clinical features identified miR-30a-5p and miR-194-5p as significantly differentially expressed between cases and controls. MiR-30a-5p is one of several microRNAs that can regulate the expression of the brain-derived neurotrophic factor

(*BDNF*) gene. Indeed, in a mouse model used to approximate binge drinking, overexpression of miR-30a-5p in the prefrontal cortex was associated with downregulation of *BDNF* expression and increased alcohol consumption [41]. The replication and observed effect size suggest that miR-30a-5p expression differences associated with behaviors like alcohol use may follow conserved biological networks, be replicable across multiple species, and provide insight into interindividual differences in health outcomes. MiR-194-5p also was significantly differentially overexpressed in young people reporting high alcohol consumption rates, and this miRNA was the highest-degree node in the miRNA network, correlating highly with the other miRNAs in this cluster. Moreover, the effect size for these two miRNAs was substantial, suggesting a robust association. A functional analysis of the miRNAs belonging to this cluster implicated 25 biological functions, with the most significant terms related to cell differentiation, inflammation, aging, epithelial-mesenchymal transition, osteogenesis, apoptosis, immune response, and onco-miRNAs. Overall, our research suggests that alcohol consumption, even in young people, may affect the expression of circulating exosomal microRNAs and cellular regulatory mechanisms. Indeed, it is possible that dysregulated alcohol consumption may affect the production of critical factors and proteins like *BDNF* throughout the body, leading to a neurobiological landscape with elevated risks for psychiatric and substance use disorders.

By examining the microRNA profiles of circulating EVs in an adolescent and young adult cohort, this study addresses several

Table 2. Linear model parameter estimates for Alcohol Use (AU) Group and covariates on expression levels of miRNA-30a-5p, miR-194-5p, and miR-339-3p.

Parameter	B	SE	t	p value	95% CI		Partial η^2
					Lower Bound	Upper Bound	
mir-30a-5p							
Sex	0.11	0.15	0.73	0.473	-0.20	0.42	0.02
Age	-0.01	0.07	-0.08	0.938	-0.15	0.14	0.00
Smoking Behaviors	0.24	0.21	1.15	0.258	-0.18	0.65	0.04
Depression Symptoms	0.01	0.02	0.37	0.713	-0.03	0.04	0.00
Twin Relatedness	0.00	0.01	0.02	0.985	-0.02	0.02	0.00
AU Group	0.66	0.19	3.50	0.001	0.28	1.04	0.26
mir-194-5p							
Sex	-0.14	0.10	-1.37	0.179	-0.35	0.07	0.05
Age	-0.06	0.05	-1.22	0.230	-0.16	0.04	0.04
Smoking Behaviors	0.07	0.14	0.47	0.638	-0.22	0.35	0.01
Depression Symptoms	-0.01	0.01	-0.41	0.687	-0.03	0.02	0.01
Twin Relatedness	-0.01	0.01	-0.92	0.365	-0.02	0.01	0.02
AU Group	0.43	0.13	3.32	0.002	0.17	0.69	0.24
mir-339-3p							
Sex	-0.05	0.10	-0.52	0.608	-0.25	0.15	0.01
Age	-0.04	0.05	-0.93	0.358	-0.14	0.05	0.02
Smoking Behaviors	0.12	0.13	0.86	0.395	-0.16	0.39	0.02
Depression Symptoms	0.00	0.01	0.15	0.880	-0.02	0.03	0.00
Twin Relatedness	0.00	0.01	-0.31	0.756	-0.02	0.01	0.00
AU Group	0.28	0.12	2.25	0.031	0.03	0.53	0.13

**Fig. 3** Comparison of Alcohol Use groups (controls versus cases) for neuron-enriched EVs miRNA-30a-5p, miR-194-5p, and miR-339-3p expression.

important gaps in the literature. First, it provides evidence that ample EVs circulate in the peripheral blood of healthy young people to justify pursuing additional work to characterize not only the roles of EVs during adolescence but also in-depth fundamental analyses to evaluate the variability of EVs number, size, type, and cargo in healthy, typically developing individuals. More research is needed to understand how biological factors (e.g., sex), genetic variation, behavior (e.g., substance use), health status (e.g., HIV status), environmental factors (e.g., exposure to pollution) and demographic factors (e.g., race, age) impact EV cargo, quantity, and destinations. Such foundational knowledge would bolster future translational work to assess the utility of EVs in clinical applications like screening tests, prognostic indicators, and precision medicine initiatives.

Second, this study indicates that high throughput omics technology like next-generation sequencing platforms to identify and quantify both known and novel RNA cargo may be feasible approaches for future EVs miRNA research in adolescents and young people based on the total amount of EVs RNA available in a modest plasma sample. In our cohort, we were able to extract 181.2 ± 42.1 ng of total RNA from the neuron-enriched EVs of each blood sample. Given that this small amount of RNA cannot be applied for the next-generation sequencing analysis, we opted to use a commercially available qPCR serum/plasma-focused panel to measure the microRNAs expression. This platform is affordable and generates modest amounts of count data that do not require specialized data wrangling skills or computer clusters to manage.

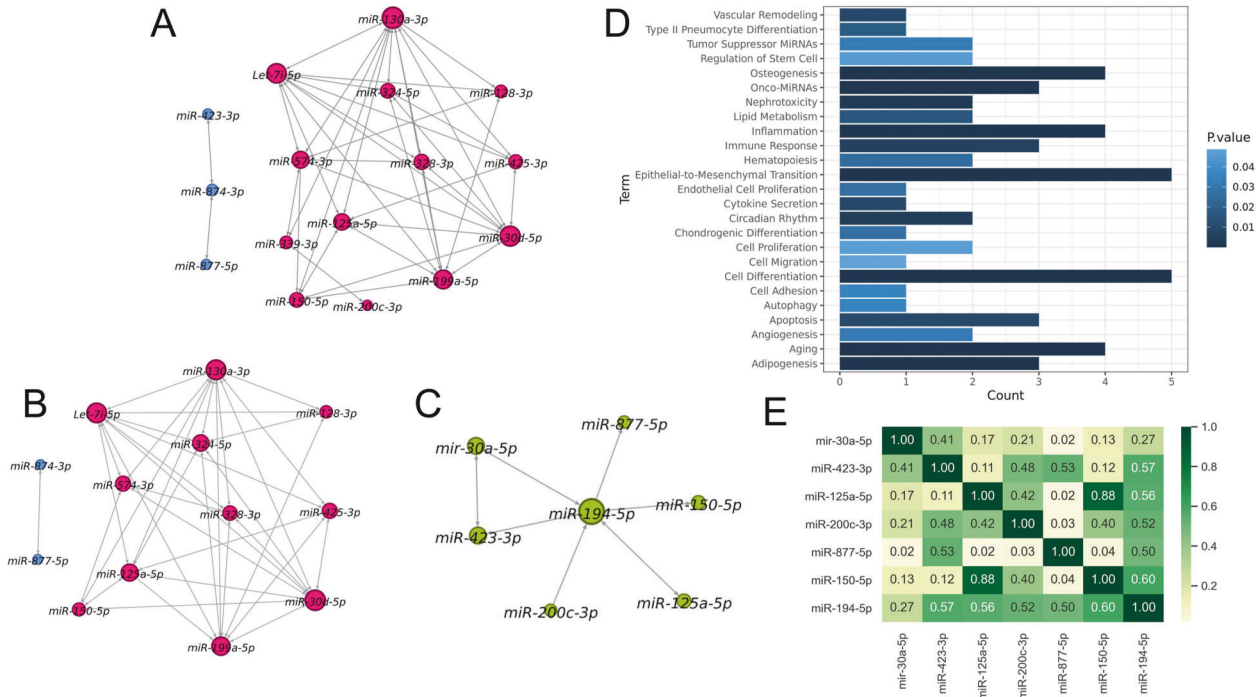


Fig. 4 MiRNA-miRNA interaction network inference. **A** Inferred miRNA-miRNA interaction network. This network consists of 16 miRNAs and 77 edges and two clusters. **B** Inferred miRNA-miRNA interaction network after dropping the twin participants. This network consists of 13 miRNAs and 69 edges and two clusters. **C** Differentially expressed miRNAs and their direct regulators consist of seven miRNAs. **D** Functional analysis of the seven miRNAs from (C) comprising two differentially expressed miRNAs and their direct regulators. The count represents the number of miRNAs within a set associated with a specific pathway. 25 biological functions are statistically significant. **E** Correlation between differentially expressed miRNAs and their direct regulators. miR-194-5p is highly correlated with the other miRNAs in this cluster.

Table 3. The number of total gene and alcohol dependence associated gene targets for each miRNA from cluster shown in Fig. 4C.

miRNA	Number of gene targets	Number of alcohol dependence associated gene targets
mir-30a-5p	1576	34
miR-423-3p	17	0
miR-125a-5p	931	12
miR-200c-3p	1196	21
miR-877-5p	131	4
miR-150-5p	356	4
miR-194-5p	473	10

However, a qPCR method is not an ideal approach for quantifying novel or unexpected RNAs because qPCR and microarrays only measure RNAs represented by the probe set. Thus, any microRNA present in a sample but unaccounted for in the microarray probe set will go unmeasured. Other work in adult populations suggest that additional noncoding RNA species may be present and in need of characterization.

Third, this study provides evidence that precipitation with Anti-L1CAM Abs is an effective and reliable method of enrichment of L1CAM-associated EVs from the human plasma samples. Previously, Norman et al. (2021) expressed concern that most of the L1CAM observed in EV studies was soluble protein not associated with EVs in CSF or plasma [71]. While we cannot speak to CSF, we demonstrated that L1CAM protein is located mainly in the EV fraction and not in the fraction of free plasma proteins (Fig. 1). Our work cannot give a clear explanation of this discrepancy. The probable reason is different approaches to EVs isolation from plasma and/or blood sample handling. Possibly, damage to EVs during certain extraction methods or improper storage of plasma

samples could lead to the release of L1CAM protein from EVs into the fraction of free plasma proteins. Additionally, although we do not have EV tracking data to confirm our L1CAM-enriched sample was primarily of neuronal origin, we are encouraged by both our own results and other findings in the literature that have identified miRNAs and proteins associated with brain disorders and brain cell activity. Collectively, these reports support the hypothesis that L1CAM is indicative of neuronal origin and that selecting EVs based on L1CAM association enriches the analytic sample for EVs of brain cell origin. Regardless of the accuracy of the L1CAM hypothesis, we strongly encourage future work characterizing L1CAM-associated EVs and suggest that even if L1CAM is not a definitive marker of neuronal origin, it has been an informative marker with relation to several mood and neuro-related disorders (e.g., Alzheimer's, Parkinson's, amyotrophic lateral sclerosis [ALS], brain injury, bipolar depression) and that this utility remains regardless of L1CAM's specificity to neurons/neural tissue [37, 72–75].

This study is not without limitations. First, despite being one of the largest studies of healthy young people, the sample size is

modest and relatively homogeneous in genetic background and socio-demographic variables like age and race. A larger, more diverse cohort is needed to explore possible age, sex, and race/ethnic related effects, and twin studies may be needed to achieve accurate estimates of the magnitude of genetic and environmental influences on EV quantity and cargo composition. Second, while the two-pronged measurement strategy of group-based microarray followed by quantitative PCR minimized financial risk, it limited data resolution; individual-level microRNA measures were collected only for the microRNAs that exhibited strong group differences, meaning that microRNAs of modest effect size or that only showed differential expression in a subset of cases were likely overlooked. Third, our analyses included almost no individuals who engaged in low-to-moderate alcohol consumption, which limited our ability to perform quantitative analyses (as opposed to categorical group analyses). A larger cohort representing a continuous distribution of drinking rates (none, low, moderate, and heavy) would increase statistical power and enable more sophisticated statistical modeling techniques. Collectively, the associations observed between neuron-enriched EVs miRNAs and alcohol use suggests that high rates of alcohol consumption during the adolescent/young adult years may impact brain maturation and functioning by modulating miRNA expression.

DATA AVAILABILITY

The data and code related to this publication have been deposited to the Open Science Framework (<https://osf.io/gaw79>). The datasets generated during and/or analyzed during the current study are available from the corresponding author upon reasonable request.

REFERENCES

- Lees B, Meredith LR, Kirkland AE, Bryant BE, Squeglia LM. Effect of alcohol use on the adolescent brain and behavior. *Pharm Biochem Behav.* 2020;192:172906.
- Carpenter RW, Treloar Padovano H, Emery NN, Miranda R Jr. Rate of alcohol consumption in the daily life of adolescents and emerging adults. *Psychopharmacol (Berl).* 2019;236:3111–24.
- Baranger DAA, Demers CH, Elsayed NM, Knodt AR, Radtke SR, Desmarais A, et al. Convergent evidence for predispositional effects of brain gray matter volume on alcohol consumption. *Biol Psychiatry.* 2020;87:645–55.
- Conteras A, Polin E, Miguens M, Perez-Garcia C, Perez V, Ruiz-Gayo M, et al. Intermittent-excessive and chronic-moderate ethanol intake during adolescence impair spatial learning, memory and cognitive flexibility in the adulthood. *Neuroscience.* 2019;418:205–17.
- Costello EJ, Mustillo S, Erkanli A, Keeler G, Angold A. Prevalence and development of psychiatric disorders in childhood and adolescence. *Arch Gen Psychiatry.* 2003;60:837–44.
- Johnston L, Miech R, O'Malley P, Bachman J, Schulenberg J. *Monitoring the future national survey results on drug use, 1975–2017: overview, key findings on adolescent drug use.* (Institute for Social Research, 2018).
- Salmanzadeh H, Ahmadi-Soleimani SM, Pachenari N, Azadi M, Halliwell RF, Rubino T, et al. Adolescent drug exposure: a review of evidence for the development of persistent changes in brain function. *Brain Res Bull.* 2020;156:105–17.
- Shen Q, Heikkinen N, Karkkainen O, Grohn H, Kononen M, Liu Y, et al. Effects of long-term adolescent alcohol consumption on white matter integrity and their correlations with metabolic alterations. *Psychiatry Res Neuroimaging.* 2019;294:111003.
- Tervo-Clemmens B, Quach A, Calabro FJ, Foran W, Luna B. Meta-analysis and review of functional neuroimaging differences underlying adolescent vulnerability to substance use. *Neuroimage.* 2020;209:116476.
- Thorpe HHA, Hamidullah S, Jenkins BW, Khokhar JY. Adolescent neurodevelopment and substance use: receptor expression and behavioral consequences. *Pharm Ther.* 2020;206:107431.
- Veer IM, Jetzschmann P, Garbusow M, Nebe S, Frank R, Kuitunen-Paul S, et al. Nucleus accumbens connectivity at rest is associated with alcohol consumption in young male adults. *Eur Neuropsychopharmacol.* 2019;29:1476–85.
- O'Brien J, Hayder H, Zayed Y, Peng C. Overview of MicroRNA biogenesis, mechanisms of actions, and circulation. *Front Endocrinol (Lausanne).* 2018;9:402.
- Coleman LG Jr, Zou J, Crews FT. Microglial-derived miRNA let-7 and HMGB1 contribute to ethanol-induced neurotoxicity via TLR7. *J Neuroinflammation.* 2017;14:22.
- Crews FT, Robinson DL, Chandler LJ, Ehlers CL, Mulholland PJ, Pandey SC, et al. Mechanisms of persistent neurobiological changes following adolescent alcohol exposure: NADIA consortium findings. *Alcohol Clin Exp Res.* 2019;43:1806–22.
- Friedman RC, Farh KK, Burge CB, Bartel DP. Most mammalian mRNAs are conserved targets of microRNAs. *Genome Res.* 2009;19:92–105.
- Gorini G, Nunez YO, Mayfield RD. Integration of miRNA and protein profiling reveals coordinated neuroadaptations in the alcohol-dependent mouse brain. *PLoS One.* 2013;8:e82565.
- Kyzar EJ, Bohnsack JP, Zhang H, Pandey SC. MicroRNA-137 drives epigenetic reprogramming in the adult amygdala and behavioral changes after adolescent alcohol exposure. *eNeuro.* 2019;6:0401–19.
- Logrip ML, Barak S, Warnault V, Ron D. Corticostriatal BDNF and alcohol addiction. *Brain Res.* 2015;1628:60–67.
- Osterndorff-Kahanek EA, Tiwari GR, Lopez MF, Becker HC, Harris RA, Mayfield RD. Long-term ethanol exposure: temporal pattern of microRNA expression and associated mRNA gene networks in mouse brain. *PLoS One.* 2018;13:e0190841.
- Sinirlioglu ZA, Coskunpinar E, Akbas F. miRNA and mRNA expression profiling in rat brain following alcohol dependence and withdrawal. *Cell Mol Biol (Noisy-le-Gd).* 2017;63:49–56.
- Solomon MG, Griffin WC, Lopez MF, Becker HC. Brain regional and temporal changes in BDNF mRNA and microRNA-206 expression in mice exposed to repeated cycles of chronic intermittent ethanol and forced swim stress. *Neuroscience.* 2019;406:617–25.
- Szabo G, Lippai D. Converging actions of alcohol on liver and brain immune signaling. *Int Rev Neurobiol.* 2014;118:359–80.
- Urena-Peralta JR, Alfonso-Loeches S, Cuesta-Diaz CM, Garcia-Garcia F, Guerri C. Deep sequencing and miRNA profiles in alcohol-induced neuroinflammation and the TLR4 response in mice cerebral cortex. *Sci Rep.* 2018;8:15913.
- Zhang Y, Wei G, Di Z, Zhao Q. miR-339-5p inhibits alcohol-induced brain inflammation through regulating NF-kappaB pathway. *Biochem Biophys Res Commun.* 2014;452:450–6.
- Lewohl JM, Nunez YO, Dodd PR, Tiwari GR, Harris RA, Mayfield RD. Up-regulation of microRNAs in brain of human alcoholics. *Alcohol Clin Exp Res.* 2011;35:1928–37.
- Tapocik JD, Solomon M, Flanigan M, Meinhardt M, Barbier E, Schank JR, et al. Coordinated dysregulation of mRNAs and microRNAs in the rat medial prefrontal cortex following a history of alcohol dependence. *Pharmacogenomics J.* 2013;13:286–96.
- Guo Y, Chen Y, Carreon S, Qiang M. Chronic intermittent ethanol exposure and its removal induce a different miRNA expression pattern in primary cortical neuronal cultures. *Alcohol Clin Exp Res.* 2012;36:1058–66.
- Ignacio C, Hicks SD, Burke P, Lewis L, Szobathayne-Meszáros Z, Middleton FA. Alterations in serum microRNA in humans with alcohol use disorders impact cell proliferation and cell death pathways and predict structural and functional changes in brain. *BMC Neurosci.* 2015;16:55.
- Ignacio C, Mooney SM, Middleton FA. Effects of acute prenatal exposure to ethanol on microRNA expression are ameliorated by social enrichment. *Front Pediatr.* 2014;2:103.
- Nunez YO, Truitt JM, Gorini G, Ponomareva ON, Blednov YA, Harris RA, et al. Positively correlated miRNA-mRNA regulatory networks in mouse frontal cortex during early stages of alcohol dependence. *BMC Genomics.* 2013;14:725.
- Kuracha MR, Thomas P, Tobi M, McVicker BL. Role of cell-free network communication in alcohol-associated disorders and liver metastasis. *World J Gastroenterol.* 2021;27:7080–99.
- Skotland T, Hessvik NP, Sandvig K, Llorente A. Exosomal lipid composition and the role of ether lipids and phosphoinositides in exosome biology. *J Lipid Res.* 2019;60:9–18.
- de Rie D, Abugessaisa I, Alam T, Arner E, Arner P, Ashoor H, et al. An integrated expression atlas of miRNAs and their promoters in human and mouse. *Nat Biotechnol.* 2017;35:872–8.
- Li XH, Zhang J, Li DF, Wu W, Xie ZW, Liu Q. Physiological and pathological insights into exosomes in the brain. *Zool Res.* 2020;41:365–72.
- D'Anca M, Fenoglio C, Serpente M, Arosio B, Cesari M, Scarpini EA, et al. Exosome determinants of physiological aging and age-related neurodegenerative diseases. *Front Aging Neurosci.* 2019;11:232.
- Goetzl EJ, Boxer A, Schwartz JB, Abner EL, Petersen RC, Miller BL, et al. Low neural exosomal levels of cellular survival factors in Alzheimer's disease. *Ann Clin Transl Neurol.* 2015;2:769–73.
- Mullins RJ, Mustapic M, Goetzl EJ, Kapogiannis D. Exosomal biomarkers of brain insulin resistance associated with regional atrophy in Alzheimer's disease. *Hum Brain Mapp.* 2017;38:1933–40.
- Nilsson J, Skog J, Nordstrand A, Baranov V, Mincheva-Nilsson L, Breakefield XO, et al. Prostate cancer-derived urine exosomes: a novel approach to biomarkers for prostate cancer. *Br J Cancer.* 2009;100:1603–7.

39. Ogata-Kawata H, Izumiya M, Kurioka D, Honma Y, Yamada Y, Furuta K, et al. Circulating exosomal microRNAs as biomarkers of colon cancer. *PLoS One*. 2014;9:e92921.
40. Zetterberg H, Burnham SC. Blood-based molecular biomarkers for Alzheimer's disease. *Mol Brain*. 2019;12:26.
41. Darcq E, Warnault V, Phamluong K, Besserer GM, Liu F, Ron D. MicroRNA-30a-5p in the prefrontal cortex controls the transition from moderate to excessive alcohol consumption. *Mol Psychiatry*. 2015;20:1219–31.
42. Kallmen H, Berman AH, Jayaram-Lindstrom N, Hammarberg A, Elgan TH. Psychometric properties of the AUDIT, AUDIT-C, CRAFFT and ASSIST-Y among Swedish adolescents. *Eur Addict Res*. 2019;25:68–77.
43. Liskola J, Haravuori H, Lindberg N, Niemela S, Karlsson L, Kiviruusu O, et al. AUDIT and AUDIT-C as screening instruments for alcohol problem use in adolescents. *Drug Alcohol Depend*. 2018;188:266–73.
44. Maisto SA, Conigliaro J, McNeil M, Kraemer K, Kelley ME. An empirical investigation of the factor structure of the AUDIT. *Psychol Assess*. 2000;12:346–53.
45. Moehring A, Rumpf HJ, Hapke U, Bischof G, John U, Meyer C. Diagnostic performance of the Alcohol Use Disorders Identification Test (AUDIT) in detecting DSM-5 alcohol use disorders in the General population. *Drug Alcohol Depend*. 2019;204:107530.
46. Reinert DF, Allen JP. The alcohol use disorders identification test: an update of research findings. *Alcohol Clin Exp Res*. 2007;31:185–99.
47. Rumpf HJ, Hapke U, Meyer C, John U. Screening for alcohol use disorders and at-risk drinking in the general population: psychometric performance of three questionnaires. *Alcohol Alcohol*. 2002;37:261–8.
48. Rumpf HJ, Wohlert T, Freyer-Adam J, Grothues J, Bischof G. Screening questionnaires for problem drinking in adolescents: performance of AUDIT, AUDIT-C, CRAFFT and POSIT. *Eur Addict Res*. 2013;19:121–7.
49. Santis R, Garmendia ML, Acuna G, Alvarado ME, Arteaga O. The alcohol use disorders identification test (AUDIT) as a screening instrument for adolescents. *Drug Alcohol Depend*. 2009;103:155–8.
50. Selin KH. Test-retest reliability of the alcohol use disorder identification test in a general population sample. *Alcohol Clin Exp Res*. 2003;27:1428–35.
51. Eyre O, Bevan Jones R, Agha SS, Wootton RE, Thapar AK, Stergiakouli E, et al. Validation of the short mood and feelings questionnaire in young adulthood. *J Affect Disord*. 2021;294:883–8.
52. Thabrew H, Stasiak K, Bavin LM, Frampton C, Merry S. Validation of the mood and feelings questionnaire (MFQ) and short mood and feelings questionnaire (SMFQ) in New Zealand help-seeking adolescents. *Int J Methods Psychiatr Res*. 2018;27:e1610.
53. Turner N, Joinson C, Peters TJ, Wiles N, Lewis G. Validity of the short mood and feelings questionnaire in late adolescence. *Psychol Assess*. 2014;26:752–62.
54. Jung MK, Mun JY. Sample preparation and imaging of exosomes by transmission electron microscopy. *J Vis Exp*. 2018;131:e56482.
55. R RCT. A Language and Environment for Statistical Computing (R Foundation for Statistical Computing: Vienna, Austria, 2019). www.r-project.org/.
56. Abreu-Villaca Y, Manhaes AC, Krahe TE, Filgueiras CC, Ribeiro-Carvalho A. Tobacco and alcohol use during adolescence: Interactive mechanisms in animal models. *Biochem Pharm*. 2017;144:1–17.
57. Boden JM, Foulds JA. Major depression and alcohol use disorder in adolescence: does comorbidity lead to poorer outcomes of depression? *J Affect Disord*. 2016;206:287–93.
58. Briere FN, Rohde P, Seeley JR, Klein D, Lewinsohn PM. Comorbidity between major depression and alcohol use disorder from adolescence to adulthood. *Compr Psychiatry*. 2014;55:526–33.
59. Doubeni CA, Reed G, Difranza JR. Early course of nicotine dependence in adolescent smokers. *Pediatrics*. 2010;125:1127–33.
60. Homman LE, Perra O, Higgins K, O'Neill F. The longitudinal relationship of alcohol problems and depressive symptoms and the impact of externalising symptoms: findings from the Belfast Youth Developmental Study. *Soc Psychiatry Psychiatr Epidemiol*. 2019;54:1231–41.
61. Jackson KM, Sher KJ, Cooper ML, Wood PK. Adolescent alcohol and tobacco use: onset, persistence and trajectories of use across two samples. *Addiction*. 2002;97:517–31.
62. Marmorstein NR, Iacono WG, Malone SM. Longitudinal associations between depression and substance dependence from adolescence through early adulthood. *Drug Alcohol Depend*. 2010;107:154–60.
63. Michalis G, Bellos S, Politis S, Magklara K, Petrikis P, Skapinakis P. Epidemiology of alcohol use in late adolescence in Greece and comorbidity with depression and other common mental disorders. *Depress Res Treat*. 2019;2019:5871857.
64. Siska F, Amchova P, Kuruczova D, Tizabi Y, Ruda-Kucerova J. Effects of low-dose alcohol exposure in adolescence on subsequent alcohol drinking in adulthood in a rat model of depression. *World J Biol Psychiatry*. 2021;22:757–69.
65. Spear LP. Consequences of adolescent use of alcohol and other drugs: studies using rodent models. *Neurosci Biobehav Rev*. 2016;70:228–43.
66. Tucker JS, Rodriguez A, Dunbar MS, Pedersen ER, Davis JP, Shih RA, et al. Cannabis and tobacco use and co-use: Trajectories and correlates from early adolescence to emerging adulthood. *Drug Alcohol Depend*. 2019;204:107499.
67. Nalluri JJ, Barh D, Azevedo V, Ghosh P. miRsig: a consensus-based network inference methodology to identify pan-cancer miRNA-miRNA interaction signatures. *Sci Rep*. 2017;7:39684.
68. Nalluri JJ, Rana P, Barh D, Azevedo V, Dinh TN, Vladimirov V, et al. Determining causal miRNAs and their signaling cascade in diseases using an influence diffusion model. *Sci Rep*. 2017;7:8133.
69. Agarwal V, Bell GW, Nam JW, Bartel DP. Predicting effective microRNA target sites in mammalian mRNAs. *Elife*. 2015;4:e05005.
70. McGeary SE, Lin KS, Shi CY, Pham TM, Bisaria N, Kelley GM, et al. The biochemical basis of microRNA targeting efficacy. *Science*. 2019;366:eaav1741.
71. Norman M, Ter-Ovanesyan D, Trieu W, Lazarovits R, Kowal EJK, Lee JH, et al. L1CAM is not associated with extracellular vesicles in human cerebrospinal fluid or plasma. *Nat Methods*. 2021;18:631–4.
72. Kapogiannis D, Boxer A, Schwartz JB, Abner EL, Biragyn A, Masharani U, et al. Dysfunctionally phosphorylated type 1 insulin receptor substrate in neural-derived blood exosomes of preclinical Alzheimer's disease. *FASEB J*. 2015;29:589–96.
73. Nila IS, Sumsuzzman DM, Khan ZA, Jung JH, Kazema AS, Kim SJ, et al. Identification of exosomal biomarkers and its optimal isolation and detection method for the diagnosis of Parkinson's disease: A systematic review and meta-analysis. *Ageing Res Rev*. 2022;82:101764.
74. Shi M, Liu C, Cook TJ, Bullock KM, Zhao Y, Ginghina C, et al. Plasma exosomal alpha-synuclein is likely CNS-derived and increased in Parkinson's disease. *Acta Neuropathol*. 2014;128:639–50.
75. Si X, Tian J, Chen Y, Yan Y, Pu J, Zhang B. Central nervous system-derived exosomal alpha-synuclein in serum may be a biomarker in Parkinson's disease. *Neuroscience*. 2019;413:308–16.

ACKNOWLEDGEMENTS

The AYATS parent study was supported by NIH/NIMH R01MH101518 to the last author (RRN). AYATS received IRB approval from the Virginia Commonwealth University IRB (protocol #HM20022942). This study and VY were supported by funds from the VCU Alcohol Research Center (P50AA022537) and from the VCU Department of Psychiatry to the last author (RRN). A National Center for Advancing Translational Sciences grant (UL1TR000058) supported resources used to conduct AYATS. PR and PG were supported by the Commonwealth Health Research Board (CHRB #236-06-23) and NSF (CBET-1802588) awarded to PG. VY also was supported by the internal fund of the VCU Massey Cancer Center. Services and products in support of the research project were generated by the VCU Massey Cancer Center Microscopy Core Shared Resource, supported, in part, with funding from NIH-NCI Cancer Center Support Grant P30 CA016059.

AUTHOR CONTRIBUTIONS

RRN and VY participated in the study design. Conceptualization of the study: RRN, VY, and DL. VY and RF performed bio-molecular experiments. Data analysis: DL, PR and PG. Writing the original draft: RRN, DL, VY, PR; all other authors commented on and refined the manuscript. Data visualization: VY and PR. All authors have carefully read the paper and approved the final manuscript.

COMPETING INTERESTS

The authors declare no competing interests.

ADDITIONAL INFORMATION

Supplementary information The online version contains supplementary material available at <https://doi.org/10.1038/s41398-024-02874-3>.

Correspondence and requests for materials should be addressed to Vasily Yakovlev.

Reprints and permission information is available at <http://www.nature.com/reprints>

Publisher's note Springer Nature remains neutral with regard to jurisdictional claims in published maps and institutional affiliations.



Open Access This article is licensed under a Creative Commons Attribution 4.0 International License, which permits use, sharing, adaptation, distribution and reproduction in any medium or format, as long as you give appropriate credit to the original author(s) and the source, provide a link to the Creative Commons licence, and indicate if changes were made. The images or other third party material in this article are included in the article's Creative Commons licence, unless indicated otherwise in a credit line to the material. If material is not included in the article's Creative Commons licence and your intended use is not permitted by statutory regulation or exceeds the permitted use, you will need to obtain permission directly from the copyright holder. To view a copy of this licence, visit <http://creativecommons.org/licenses/by/4.0/>.

© The Author(s) 2024